TECHNICAL ISSUES ASSOCIATED WITH THE SEISMIC ANALYSIS OF THE SAN MATEO - HAYWARD BRIDGE

R. Donikian[1], C.-Y. Chang[2], M. Tabatabaie[3], and R. Polivka[4]

Abstract

A seismic performance evaluation of the San Mateo-Hayward Bridge has been performed for the California Department of Transportation (Caltrans). The 7 mile long structure, which is one of the major crossings in the San Francisco Bay Area, is situated approximately 7 miles from the San Andreas Fault line at the west end, and 5 miles from the Hayward Fault line at the east end. The study included the development of ground motions, consideration of SSI effects, and multiple support time history analysis. The objective of this paper is to highlight the philosophy and strategy employed for the seismic performance evaluation.

Introduction

The San Mateo-Hayward Bridge, which connects Foster City and Hayward, has a shore-to-shore alignment length of approximately 7 miles, and consists of a 1.85 mile long steel bridge at the west end connected to a 4.9 mile long concrete trestle that extends to the Hayward shore (Fig. 1). The structure is situated 6.9 miles (11 km) from the San Andreas Fault line at the west end, and 5 miles (8 km) from the Hayward Fault line at the east end. The bridge is relatively modern, as it of 1960's vintage design and construction, and was opened to traffic in 1967.

A comprehensive seismic vulnerability assessment of the bridge has recently been performed for Caltrans by Cygna Group, Inc., in association with Tudor Engineering Co., Geomatrix Consultants, Geospectra, ESE Consulting Engineers, Manna Consultants, SDV/ACCI, and Professors A. Astaneh and G. Powell of UC Berkeley. The evaluation has been conducted for a magnitude M_w 8 Maximum Credible Earthquake (MCE) associated with the San Andreas fault system, which has been determined to govern over the Hayward event. This paper highlights

[1] Technical Specialist, Cygna Group, Inc., 1800 Harrison St., Oakland, CA. 94612.
[2] Vice President, Geomatrix Consultants, Inc., 100 Pine St., San Francisco, CA. 94111.
[3] Vice President, Geospectra, Inc., 3095 Atlas Rd., Suite 213, Richmond, CA. 94806
[4] Vice President, Cygna Group, Inc., 1800 Harrison St., Oakland, Ca. 94612.

the significant modeling and analytic challenges posed by the extensive alignment length and the variability of the subgrade conditions and ground motions. The performance evaluation strategy was developed on the basis of the following objectives in mind: (1) obtaining realistic estimates of displacements and deformations; (2) obtaining realistic estimates of seismic demand loads; and (3) developing structural component performance criteria in terms of deformation.

Bridge Structural Configuration

The steel bridge alignment is approximately 1.85 miles long, and has both horizontal and vertical curvature. The structure comprises 18 anchor units connected by suspended spans in an alternating sequence as depicted in Fig. 1 and 5. These anchor units consist of a double pier unit supporting the superstructure on pin bearings. The suspended spans are supported by eye-bars from the cantilevered deck box girder sections of the anchor units. These eye-bar connections constitute the hinges in the system with an alternating sequence of tied hinges at one end, and expansion hinges with rod restrainers at the other end of the suspended units. The anchor unit spans are 208 feet long on the low rise sections of the bridge, and 292 feet in the low- to intermediate rise sections. The main center span has a length of 750 feet over the main navigation channel, and a vertical clearance of 165 feet above the waterline.

The deck structure consists of a dual steel box-girder orthotropic deck superstructure supported by pin bearings on dual steel and concrete towers connected by spandrel beams. The portal frame tower legs are supported by a substructure consisting of 38 concrete piers supported on steel H-pile foundations throughout the alignment. The water depth varies from 5 to 17 feet between piers 2-13, & 30-38, and 50-65 feet between piers 17-28. The steel tower legs consist of 12'x10' rectangular sections of cellular construction, and the concrete towers consist of rectangular 12'x4' sections.

The substructure piers consist of dual reinforced concrete rectangular columns (typically 11'x4') and hollow shafts (18 ft diameter with 3'-2" walls) connected by spandrel beams. The longitudinal reinforcement consists typically of #11 bars, and transverse reinforcement of #6 ties 9" on center. The concrete piers are supported on pile foundations consisting of steel H-pile groups of rectangular and "bell" type configurations throughout the alignment. Typical pile tip elevations are at 250 ft below the waterline.

The trestle consists of an articulation of 857 simple spans, constructed out of reinforced concrete precast deck and bent elements supported on a row of 80-foot long prestressed concrete piles spaced 30 feet apart. The piles are spirally reinforced prestressed hollow shafts of 24 inch diameter, driven through a layer of soft Bay Mud, varying in thickness between 20 to 50 feet, into the relatively stiff alluvium. The water depth along the entire trestle alignment is approximately 5 feet.

Site Geology and Ground Motions

The subsurface soil conditions at the site consist of soft to medium stiff clays (Bay Mud) that extend to depths of approximately 50 feet below the mudline (Fig. 2). The Bay Mud layer is underlain by alternating layers of cohesionless soils (sands, sandy silts), and cohesive soils

(clays, clayey silts). These unconsolidated sedimentary deposits reach estimated depths of 600 to 700 feet below the waterline. Available soil boring data indicates that sandstone bedrock was encountered at a depth of about 55 feet below the mudline at Pier 1, and depths to bedrock at other pier locations are unknown.

The ground motions (developed by Geomatrix Consultants) consist of an incoherent wavefield, representing the MCE, defined by motions at 11 pier locations: Piers 1, 4, 9, 13, 16, 19, 20, 24, 28, 32, and 38. These motions reflect the following effects: (a) seismic wave passage effects associated with wave arrival time differences at different stations; (b) incoherence effect due to wave superposition, reflection and scattering; and (c) variability of soil column along the alignment. The free-field mudline motion in the longitudinal direction at Pier 20, and mudline acceleration response spectra at piers 1,4,9,16,19,20,24 are shown in Fig. 3 & 4.

These ground motions were developed using nonlinear and equivalent linear site response analysis techniques. The vertical motions were developed using equivalent linear technique (SHAKE) without degradation of compressional-wave velocities with level of excitation. The horizontal motions were developed using a modified version of DESRA, which is a dynamic effective stress nonlinear analysis code. Soil profiles and dynamic soil properties at each of the 11 pier locations were developed based on available soil boring logs, soil test data, and other published data for similar soils in the San Francisco Bay. To assess the effects of the sloping rock boundary on the ground motion near the east end of the bridge, a two-dimensional model of the soil deposits was developed. The analysis results appear to indicate that, except for Piers 1 and 4 (near the edge of the model), 2D effects are small at other pier locations. The 2D effects were incorporated in generating the motions at Pier 1 and 4.

Structural Component Performance Criteria

The seismic performance assessment has been conducted in terms of the structural component performance criteria on the basis of the following considerations:

Steel Structural Elements Inelastic response is assessed in terms of available *load ductility* levels as measured by interaction relations. For bending, the interaction relation is a function of axial load and biaxial moment (P-M-M), and for shear, the interaction ratio is a function shear and moment. The following interaction equation was derived by A. Astaneh (Cygna Report, 1993) for the steel column elements:

$$P/(aP_y) + [M_l/(bM_{pl})]^2 + [M_t/(cM_{pt})]^2 \leq R^2 \quad (1)$$

where: P = axial load; P_y = axial yield capacity; M_l, M_t = applied moments in the longitudinal and transverse directions; M_{pt} , M_{pl} = plastic moment capacities in pure bending in the transverse and longitudinal directions; a, b, c = reduction factors for axial strength, and plastic moment capacities in the longitudinal and transverse directions; and R = Response modification factor.

The response modification factor, R, is defined as the ratio of the elastic force response to

the force response at the point of significant yield. The allowable levels of the R-factor developed for the steel flexural elements in the bridge range from 1.5 to 5. These levels were substantiated by nonlinear finite element analyses, using the fiber elements in DRAIN-3DX.

Concrete Members The performance criteria for the evaluation of the reinforced concrete flexural members are in terms of *displacement ductilities*. For the duration and intensity of the scenario earthquake expected at the site, the performance of plastic hinge cycling in the inelastic range can only be assessed in terms of deformation analyses. For comparison purposes, load based demand capacity ratios (Z factors) were also computed and found to be unreliable measures of performance. For the trestle piles, load displacements curves of the soil-pile system were developed to assess pile performance. Deformation-based performance criteria and shear capacities of the concrete components are computed using M.J.N. Priestley's recommended method (Priestley, 1991).

Foundation Performance Criteria Foundation performance was evaluated on the basis of load-displacement curves developed (by Geomatrix) for the foundation soil-pile groups. Similar curves were developed for the evaluation of the trestle piles.

Dynamic Analyses

A comprehensive set of linear and nonlinear dynamic analyses were conducted to assess the seismic performance of the steel structure and the concrete trestle. Due to differences in structural system, subsurface conditions, foundation configuration, and boundary interaction effects, the steel structure and concrete trestle were treated separately in this study. To properly assess the global seismic response of extended structures of this size, multiple support excitation analyses are required. In addition, the variation of ground motion intensities and subsurface conditions along the alignment of this structure are quite significant. The basic form of the governing equations of motion for multiple support seismic excitation are given by (Clough and Penzien, 1975)

$$\mathbf{M}\,\ddot{\mathbf{v}}^t = -\mathbf{C}\,\dot{\mathbf{v}}^t - \mathbf{K}\,\mathbf{v}^t + \mathbf{F} \tag{2}$$

where $$\mathbf{v}^t = \begin{bmatrix} \mathbf{x}_t \\ \mathbf{u} \end{bmatrix} = \begin{bmatrix} \mathbf{x} + \mathbf{x}_s \\ \mathbf{u} \end{bmatrix}$$

in which: $\mathbf{u}$ = support dof's; $\mathbf{x}$ = dynamic dof's; $\mathbf{x}_s = \mathbf{R}\,\mathbf{u}$; pseudostatic displacement vector; and $\mathbf{R} = -\mathbf{K}_{ss}^{-1}\,\mathbf{K}_{sb}$ (see Eq. (3)). Using these, the expanded form of Eq. (2) is given by

$$\begin{bmatrix} \mathbf{M}_{ss} & \mathbf{M}_{sb} \\ \mathbf{M}_{bs} & \mathbf{M}_{bb} \end{bmatrix} \begin{bmatrix} \ddot{\mathbf{x}}_t \\ \ddot{\mathbf{u}} \end{bmatrix} + \begin{bmatrix} \mathbf{C}_{ss} & \mathbf{C}_{sb} \\ \mathbf{C}_{bs} & \mathbf{C}_{bb} \end{bmatrix} \begin{bmatrix} \dot{\mathbf{x}}_t \\ \dot{\mathbf{u}} \end{bmatrix} + \begin{bmatrix} \mathbf{K}_{ss} & \mathbf{K}_{sb} \\ \mathbf{K}_{bs} & \mathbf{K}_{bb} \end{bmatrix} \begin{bmatrix} \mathbf{x}_t \\ \mathbf{u} \end{bmatrix} = \begin{bmatrix} \mathbf{0} \\ \mathbf{F}_b \end{bmatrix} \tag{3}$$

in $\mathbf{M}$, $\mathbf{C}$, and $\mathbf{K}$ are the mass, damping, and stiffness matrices, respectively, and the subscripts "s" and "b" denote "structure" and "base" respectively. For structural dynamics software without multiple support excitation capabilities, the implementation of these equations requires

e use of very stiff springs connected coaxially with foundation springs. The seismic excitation then input in terms of forces (F_b) appropriately scaled to reproduce the ground motions, via e stiff boundary springs, and applied at the foundation spring interface.

The dynamic analyses were conducted using Prof. Ed Wilson's Ritz method-based SADSAP omputer program, and DRAIN-3DX developed at UC Berkeley under the direction of Prof. G. owell. The mudline motion displacement time histories were used as the excitation (i.e. no scattering effects were considered) for the analyses. Due to the unavailability of the multiple support displacement input option in the SADSAP version used, the stiff boundary spring technique cited above was used. To account for the motions at the piers for which ground motions are unavailable, the motions generated at the 11 pier locations were "smeared" using influence functions for the multiple support excitation analyses. In the SADSAP analyses, this is readily accomplished via the specification of Ritz vectors.

Finite Element Models

Steel Structure The finite element discretization of the steel structural model is shown in Fig. 8. This model consists of almost 6000 degrees of freedom, and is assembled using the deck super-elements discussed below. Various models were generated to simulate the following effects: (a) dynamic response due to multiple support excitation; (b) variability of the ground motions along the bridge alignment; (c) soil-structure interaction; and (d) expansion hinge nonlinearities and variations in gap stiffness. The salient features of the models are discussed below.

Dual Box-Girder Deck Behavior: A super-element representing the dual box-girder deck units has been developed to properly the behavior of the deck. Due to the concentration of stiffness on the box-girders, the potential for independent box-girder vibration has been assessed and simulated.

Reinforced Concrete Flexural Members: The reinforced concrete flexural member stiffness properties, moment capacities, and displacement and curvature ductilities have developed on the basis of moment curvature analyses. The elastoplastic idealization adopted, shown in Fig. 6, is based on: (a) section moment curvature analysis; (b) yield point defined as onset of longitudinal steel yield or concrete strain of .002; (c) ultimate curvature and displacement; and (d) curvature and displacement ductility.

Expansion Hinges: For the nonlinear analyses, the expansion hinge nonlinearities are modeled using a combination of three parallel spring elements. This system comprises: (a) a tension only element representing the hinge restrainers; (b) a gap element representing the gap between the suspended span deck and the anchor unit deck; and (c) the linear "gravitational" spring due to the pendular displacement kinematics of the suspended eye-bars.

SSI Model: The "soil-foundation" interaction component of the "soil-foundation-structure" effect were modeled by performing SSI analyses of the soil-foundation system using the SASSI computer program. The SSI analyses were performed (by Geospectra Inc.) to derive foundation impedance matrices which were used to develop 6x6 stiffness and damping matrices representing

the soil-pile group system for each foundation type. Fig. 7 shows an isometric view of the SSI models used in the SASSI analyses. The foundations consist of a group of steel H-piles connected by a tremie seal (concrete pile cap). The soil model consists of a viscoelastic layered system underlain by a uniform halfspace (bedrock). The soil properties were obtained from one-dimensional free-field soil column studies that included densities and strain compatible shear-wave and compressional-wave velocities, and damping ratios.

In this model, the pile cap was modeled as a rigid, massless block using solid elements. The near-field soils were included explicitly in the foundation model by 3D soil elements, and piles were modeled using three-dimensional beam elements. The pile elements were rigidly connected to the pile cap at the top and extended into the soil layers. In addition to the stiffness component of the impedance, the foundation damping properties were also developed, including both material and radiation damping. Due to very small coupling between the rocking and sliding stiffnesses in this case, the foundation springs were readily implemented using translational and rotational springs in the structural model.

Concrete Trestle The concrete trestle was analyzed using multiple support time history analyses. Due to the unavailability of a set of motions representing the incoherent wave field, the excitation has been simulated by propagating the ground motions developed for Pier 38 down the trestle alignment with a constant time delay. Due to the presence of expansion joints at every bent DRAIN-3DX nonlinear finite element models, using super-element representations of each repetitive unit, were used to analyze the response. The models developed included several variations incorporating the following effects: (a) models with variable number of spans; (b) soil-pile kinematics; and (c) expansion hinge nonlinearities. Several models with varying number of spans (7, 20, 60, and 200) have been used for the analyses, to assess local and global behaviors. The soil-pile system stiffnesses were computed on the basis of a typical soil-pile configuration. These problem sizes ranged from under 1000 dof's to 15,000 dof's.

Response Analyses

A variety of dynamic analyses were performed to assess the seismic response of the structure in terms of displacement, deformation, and load demands. The following three types of models were used in the analyses: (a) Type 1: linear elastic "tension" models with expansion hinges modeled as two-way tension-compression elements; (b) Type 2: models incorporating the limited nonlinearities associated with expansion hinges. The hinges were modeled using tension-only restrainer elements and compression-only gap elements. These were used for multiple support excitation time history analyses; and (c) Type 3: general nonlinear models incorporating both expansion hinge nonlinearities and material nonlinearities associated with plastic hinges.

The types of analyses conducted consist of: (a) Uniform Response Spectrum (URS) Analyses with the objective of obtaining preliminary seismic demand estimates and perform parametric studies; (b) Multiple Support Time History (MSTH) Analyses consisting of a series of multiple support time history analyses with the objective of obtaining realistic estimates of displacements and deformations in the structure; and (c) Uniform Base Time History (UTH) Analyses, mainly performed for calibration purposes to serve as a tool for comparing results obtained by the URS and MSTH analyses. They UTH analyses have also proven useful in quantifying the effects of

strong nonlinearities exhibited by expansion hinges, and ground motion propagation effects via time delays.

The analyses included sensitivity studies to assess the effects of variations in parameters such as foundation stiffness, expansion hinge behavior, and the significance of multiple support excitation. Some of the significant results obtained from the dynamic analyses of the steel structure are highlighted here. Fig. 9 shows Pier 16 tower drift (with respect to foundation footing) obtained for the MSTH, UTH-20 (UTH with Pier 20 motions), and UTH-20D (Pier 20 motions propagated down the alignment--Pier 1 to 38--with appropriate time delays) analysis cases. These results indicate that the variability of ground motions along the bridge alignment has a significant effect on structural response, and that response due to multiple support excitation (MSTH) seems to be closely related to response due to time delay effects of propagating ground motions (UTH-20D). Fig. 10 depicts the response of the expansion hinge at the suspended unit 15-16, for the MSTH analysis case. It is clear from these results that expansion hinge behavior must be properly modeled to obtain realistic seismic demand estimates.

Conclusions

For vulnerability assessments of large structures, such as this one, with strong nonlinearities due to expansion hinges, MSTH type of analysis is the rational alternative to the much too conservative uniform response spectrum method, which is more of a design tool rather than a diagnostic one. The following conclusions were drawn from the study: (1) load based criteria (Z-factors) are unreliable for concrete components; (2) deck restrainers and expansion hinge behavior play a major role in the performance of the superstructure; (3) effects due to multiple support excitation are significant. Specifically, there is significant reduction in demand compared to estimates obtained by conventional uniform response spectrum analyses. However, in some cases the demand on some components may be higher compared to uniform time history excitation cases; and (4) uncertainties such as foundation stiffness and ground motion variabilities must be carefully assessed for structural response analyses of large structures.

Acknowledgements

Many people were involved in this project. We would like to extend our thanks to Stan Larsen and Mark Yashinsky of Caltrans for their guidance, the project staff at Cygna, Tudor, Geomatrix, Geospectra, ESE, Manna, and SDV/ACCI for their outstanding effort in producing the interesting results that were obtained, and to Professors Astaneh, Powell, and Wilson, for all the advice and state-of-the-art software and information they provided.

References

Cygna Report No. 930160. "Seismic Analysis of the Existing San Mateo Bridge", Rev. 0, October 1993.

Clough, R., and J. Penzien. *Dynamics of Structures*. McGraw-Hill, 1975.

Priestley, M.J.N. "Seismic Assessment of Existing Concrete Bridges", UC San Diego Dept. of AMES Report No. SSRP-91/03, July 1991.

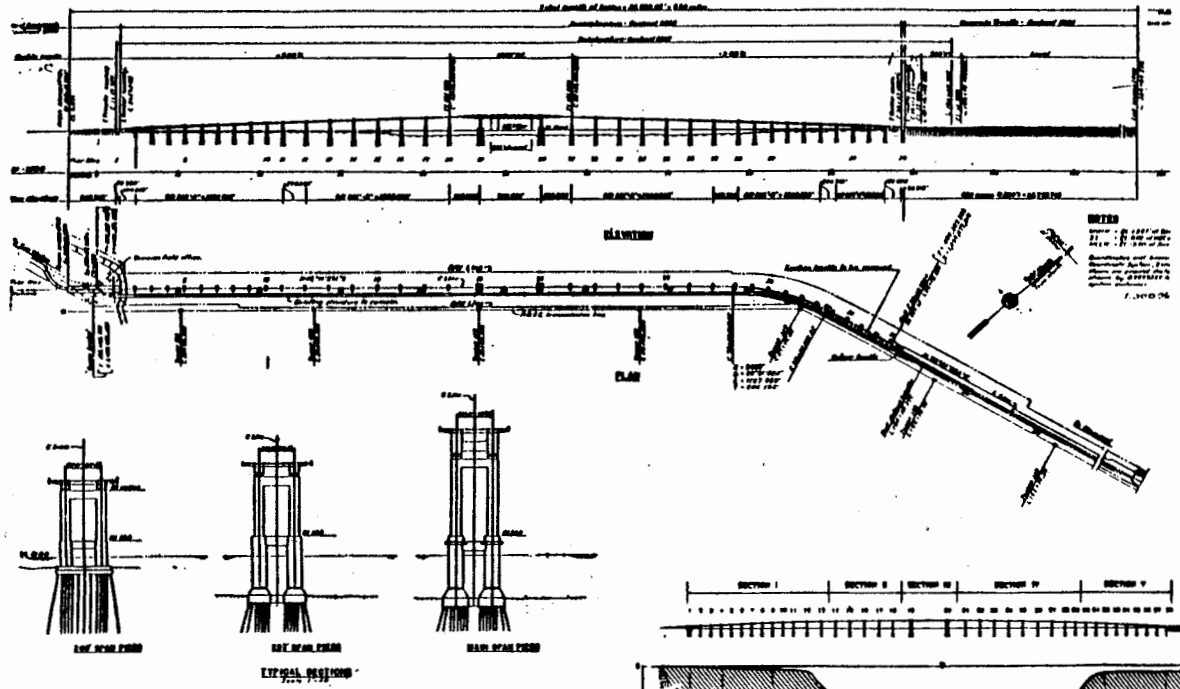

Fig. 1 San Mateo-Hayward Bridge General Plan

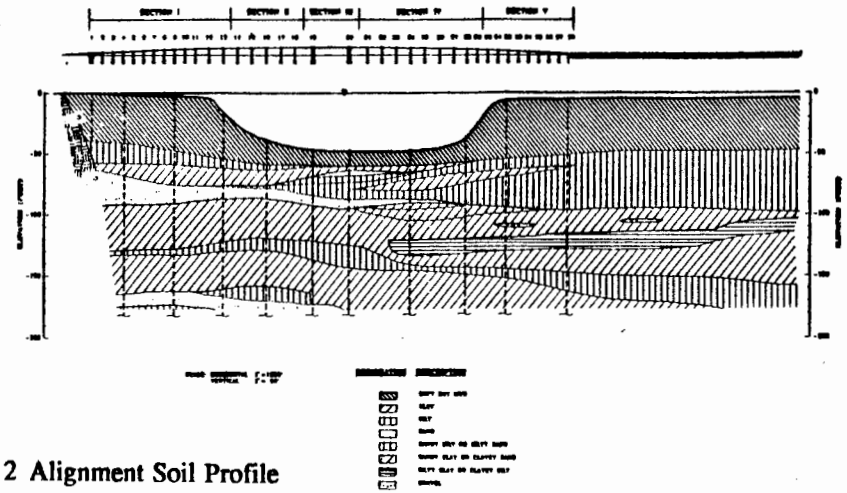

Fig. 2 Alignment Soil Profile

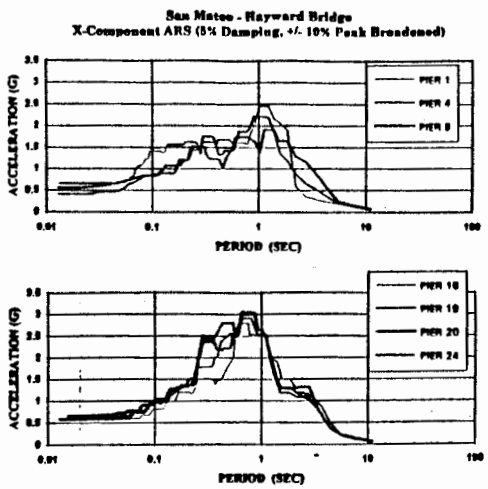

Fig. 3 Mudline Acceleration Response Spectra

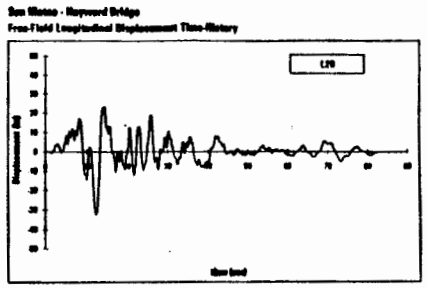

Fig. 4 Pier 20 Mudline Displacement

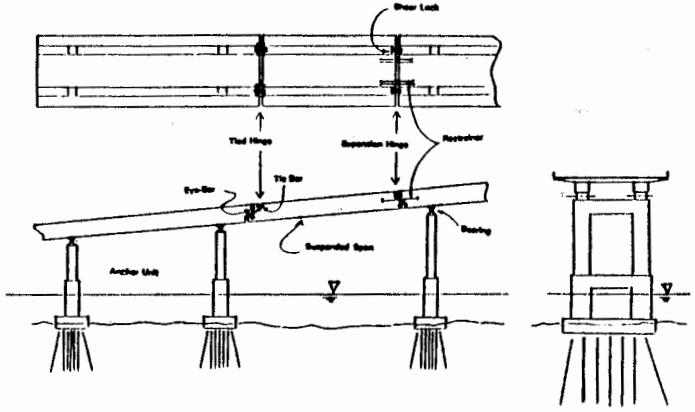

Fig. 5 Steel Bridge Structural Configuration

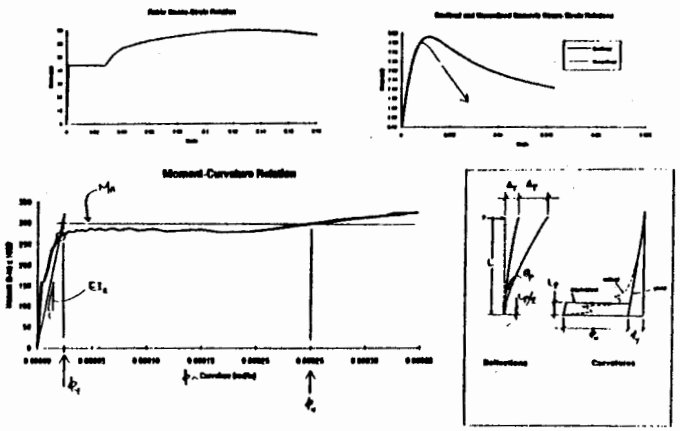

Fig. 6 Reinforced Concrete Member Model

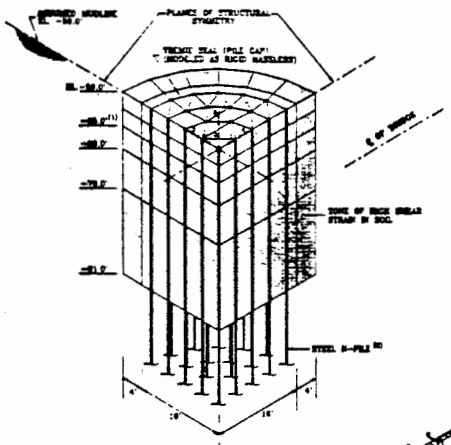

Fig. 7 Steel Bridge
Foundation SSI Model

Fig. 8 Steel Bridge Finite Element Model

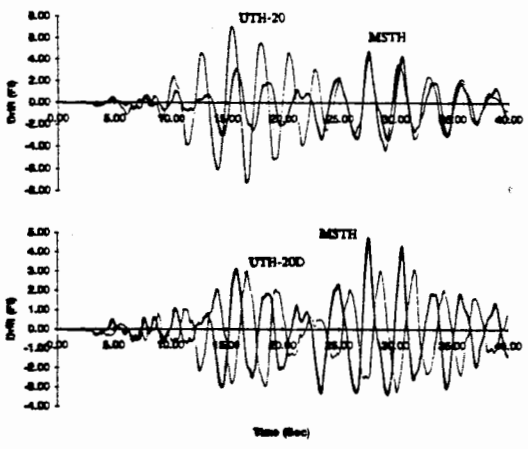

Fig. 9 Pier 16 Tower Drift (wrt Foundation)

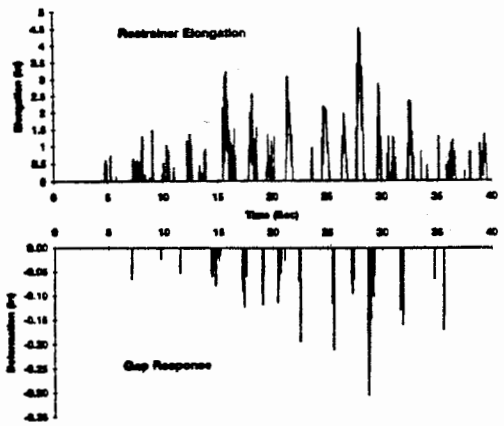

Fig. 10 Suspended Unit 15-16
Expansion Hinge Response